

## STUDIES OF SURFACE PROPERTIES OF PURE AND MODIFIED BY $Mn^{2+}$ AND $Ni^{2+}$ IONS OF ALUMINIUM OXIDE SAMPLES USING COMPLEX METHODS

P. Staszczuk<sup>1\*</sup>, M. Majdan<sup>2</sup>, S. Pikus<sup>3</sup>, D. Sternik<sup>1</sup> and M. Błachnio<sup>1</sup>

<sup>1</sup>Department of Physicochemistry of Solid Surface, Chemistry Faculty, Maria Curie-Skłodowska University  
M. Curie-Skłodowska Sq. 3, 20-031 Lublin, Poland

<sup>2</sup>Department of Inorganic Chemistry, M. Curie-Skłodowska Sq. 2, 20-031 Lublin, Poland

<sup>3</sup>Department of Crystallography, M. Curie-Skłodowska Sq. 3, 20-031 Lublin, Poland

Complex studies of physicochemical properties of pure and modified of alumina oxides samples are presented. The presence of  $Mn^{2+}$  and  $Ni^{2+}$  modifiers on the aluminium oxide surface causes increase in water adsorption capacity and decrease in benzene and *n*-octane adsorption. This is due to decrease of specific surface area, volume and radius of pores as a result of surface impregnation and microcrystal formation during modification with manganese and nickel chlorides. Microcrystal formation on the surface and porosity decrease as confirmed by AFM, EDX and powder diffraction studies using automated diffractometer by step scanning.

From the Q-TG and Q-DTG data, the energies of liquid desorption from the surface of the samples and the functions of desorption, energy distribution were calculated. High degree of nonlinearity of the functions resulting from great heterogeneity of the studied surface was found. Adsorption of cations creates more homogeneous surface in aluminium oxide, and it is responsible for the change in adsorbate molecule interaction energy and changes mechanism of adsorption and desorption as well as thickness and structure of the adsorbed film. From the experimental data some parameters characterizing adsorption properties and porosity of the studied samples were determined using the complex measuring methods (thermal analysis, sorptometry, porosimetry, AFM and EDX).

**Keywords:** adsorption of ions, aluminium oxides, desorption energy, fractal dimensions, surface properties, thermogravimetry Q-TG

### Introduction

Defects in the structure formed during dehydroxylation create active adsorption and catalytic centres. Various properties of aluminium oxide surfaces and the presence of different types of hydroxide groups of various concentrations enable modification using a variety of methods. Thermal dehydroxylation is a single method for aluminium oxide surface modification. Physically bonded water is removed during sample drying and surface dehydroxylation takes place at high temperatures (about 1000°C). Chemical nature of active centres responsible for the phenomenon of adsorption is not yet completely known.

Aluminium oxide surfaces are modified in order to apply for separation of mixtures and as catalysts in many industrial processes. A main task is to increase selectivity of adsorption on the surface of individual compounds included in the mixture. A more complex way of changing properties of aluminium oxide surface is modification by addition of chemical compounds (modifiers) activating the desired active centres and deactivating the undesired ones. Addition of acids or bases affecting concentration and reactivity of surface hydroxide groups of aluminium oxide can serve as an example

of such surface modification [1]. Another method of aluminium oxide surface modification is addition of new functional groups on their surface.

To increase activity of aluminium oxide as the adsorbing substance or catalyst support, it is modified with such metal cations as Mn, Ni, Cr, Fe, Co. Physicochemical properties of the new surface (e.g. adsorption capacity, porosity) differ significantly from the primary one [2, 3]. In such modification aluminium oxide (support) is subjected to the action of the solution including an active component, i.e. metal ions [4, 5]. Excess solution not bonded with the support is removed by evaporation and the support can be of different character. The solution can be adsorbed on the support surface forming surface complexes of various types. Solution components can undergo ion exchange with surface groups or chemical reaction. Interaction forces can be relatively weak and adsorption of active component can have character of physical adsorption. Depending on the interaction type, the addition methods can be divided into adsorption, ion exchange and impregnation [6].

The amount of active component that can be spread on the support surface depends on many parameters: nature and structure of support, chemical

\* Author for correspondence: piotrs@hektor.umcs.lublin.pl

properties of active component in the solution and spreading conditions [7].

We present the results of studies on the effect of  $\text{Mn}^{2+}$ ,  $\text{Ni}^{2+}$  cations on adsorption and porosity properties of the surfaces of aluminium oxides with respect to applicability in various technological processes. The analysis of physicochemical properties of modified aluminium oxide was made from the experimental results obtained by means of derivatograph, sorptometer porosimetry as well as AFM and EDX microscopy.

## Experimental

Liquid thermodesorption measurements from the sample of commercial aluminium oxide (type Aldrich, USA) were carried out using a derivatograph Q-1500D (MOM Hungary) [8]. The Q-TG mass loss curve and Q-DTG differential mass loss curve in relation to temperature and time were measured under quasi-isothermal conditions over a 20–300°C temperature range. The curves were measured over a constant optimum heating rate of 6°C min<sup>-1</sup>. The sample was thermally treated in air at 300°C already located in the vacuum desiccator, where the relative vapour pressure of benzene was  $p/p_0=1$ . About 0.5 g of the wetted aluminium oxide was placed in the special platinum crucible of the thermogravimetric analyzer. Specific surface areas and pore volumes were determined from low-temperature nitrogen adsorption (Sorptomat Micrometrics ASAP 2405 V1.01, USA) and Porosimeter 4000 (Carlo Erba Instruments, Italy). The photographs were made by means of the atomic force microscopy NanoScope III (Digital Instruments, USA) and scanning electron micrographs were also obtained by means of the apparatus JSM-25 JOEL type and LEO SEM 1430VP with EDX detector. The powder diffraction data were collected at room temperature in the  $2\Theta$  range from 5 and 90° on a modified DRON-3.0-SEIFERT automated diffractometer by step scanning with a step equal 0.02° and a count time 6 s/step. The experimental conditions were as follows: Cu target X-ray tube operated at 45 kV and 30 mA, 6° take-off angle, 1° divergence slit, 0.15 mm receiving slit, scintillation counter with pulse height analyzer, Ni filter.

The sample to be activated, basic aluminium oxide produced by Aldrich, were used for modification and then in the programmed thermodesorption. Its characteristics are as follows: activity in Brockman – I, size of molecules (mesh): ~150, size of pores – 5.8 nm, specific surface area – 155 m<sup>2</sup> g<sup>-1</sup>, water – 1.5%, Na<sub>2</sub>O – 0.4%, Fe<sub>2</sub>O<sub>3</sub> – max. 0.02% and SiO<sub>2</sub> – max. 0.02%, no of category – 19.944-3, type – basic, pH – 9.5. The samples of active, basic aluminium oxide were subjected to the action of solu-

tions containing various concentrations of metal ions ( $\text{Mn}^{2+}$ ,  $\text{Ni}^{2+}$ ). The choice of these cations was determined by those used in industry as the adsorbent or catalyst in hydrogenation reactions and to separate gaseous mixtures like e.g. H<sub>2</sub>/Ar [9, 10]. The samples of aluminium oxide modified with ions are used as chromatographic column packings, for separation of alkenes and alkanes [11].

The samples to be studied were prepared using the impregnation method [6] consisting in spreading the active component from the solution. Active, basic aluminium oxide was sieved and then the fraction of 0.15 nm grain thickness was removed. Hydrated manganese chloride ( $\text{MnCl}_2 \cdot 4\text{H}_2\text{O}$ , analytical pure, POCH Gliwice) and hydrated nickel chloride ( $\text{NiCl}_2 \cdot 6\text{H}_2\text{O}$ , analytical pure, POCH Gliwice) were used for modification. Five 10 g portions of aluminium oxide were weighed and then placed in evaporating dishes. More information is given in paper [12].

The manganese chloride content in five samples were: 0.99; 1.94; 3.81; 5.6 and 7.34% but the nickel chloride content was 1.17; 2.32; 4.54; 6.66 and 8.68%, respectively.

Distilled water, benzene (POCH Gliwice) and *n*-octane (analytically pure, Fluka) were used for adsorption from the gaseous phase on the surface of modified aluminium oxide samples. Before measurements of thermodesorption, the samples were prepared as follows. Suitable weighed portions of aluminium oxides were dried in the furnace at 300°C for 24 h to remove hygroscopic water from their surface. Then they were placed in the vacuum desiccator containing the studied liquid where  $p/p_0=1$  and left for 24 h to establish the adsorption equilibrium. Then the samples were subjected to programmed thermodesorption measurements in the temperature range 20–300°C. The obtained results of studies of the samples with spread manganese and nickel cations were compared with analogous parameters (e.g. adsorption capacity, pore volume, surface area, fractal dimensions) obtained for the sample of pure aluminium oxide.

The curves of thermodesorption Q-TG and Q-DTG of the above mentioned liquids from the surface of individual aluminium oxide samples were recorded. From the obtained thermodesorption curves and data from the sorptometer (specific surface area size), the statistical number of liquid monolayers on the surface of studied aluminium oxides was calculated. The properties of aluminium oxide sample surfaces modified with manganese and nickel cations were determined from the programmed thermodesorption data of some liquids (water, benzene and *n*-octane) using the so-called quasi-isothermal program of derivatograph Q-1500 D. Before studies the samples were saturated with liquid vapours in the

vacuum desiccator where  $p/p_0=1$ . During such sample preparation before measurements, all surface forces were compensated by adsorbing liquid molecules.

## Results and discussion

The mass loss corresponding to the sample adsorption capacity for individual liquids obtained from the measurements of thermal analysis depending on the amount of the modifier Mn<sup>2+</sup> and Ni<sup>2+</sup> on the aluminium oxide surface are presented in Table 1. This table presents the calculated values obtained from thermal analysis measurements for the mentioned samples, the values of individual adsorption parameters (adsorption capacity,  $a$ , expressed in mmol g<sup>-1</sup> and the number of statistical liquid monolayers,  $n$ ). In the case of water adsorption the value of sample adsorption capacity increases with the concentration of modifiers. However, the presence of cations on the surface decreases adsorption capacity of aluminium oxide compared with that of benzene and *n*-octane. The greatest changes of values of water adsorption capacity were obtained for the samples of aluminium oxide with spread Mn<sup>2+</sup> and Ni<sup>2+</sup> cations of concentration of 0.4 mmol g<sup>-1</sup>. For the samples with adsorbed benzene and *n*-octane on aluminium oxide, a tendency for decreasing the amount of the liquid adsorbed on the surface of modified adsorbent (adsorption capacity) was observed. Therefore further parts of this paper will describe the results of studies for the samples of aluminium oxide with spread cations of concentration of 0.4 mmol g<sup>-1</sup> which are responsible for the greatest changes in physicochemical properties of aluminium oxide surface.

The curves of water loss, Q-TG, and their differential curves, Q-DTG, are presented in Fig. 1 for pure samples and for those covered with modifying substances (manganese and nickel chlorides of the solutions with concentrations of 0.4 mmol g<sup>-1</sup>). They are characterized by occurrence of inflexions or peaks due to gradual evaporation of liquid depending on energy of bonding of molecule in the adsorption layer with the surface and/or ions (Figs 1a–c) of the studied sample. Covering of the surface with modifiers is responsible for occurrence of inflexions on the Q-DTG curves and shift of peak minima towards higher temperatures which is a result of increase of intermolecular interaction force and energy of liquid desorption from the surface of studied samples.

From the curves Q-TG and Q-DTG, the functions of energy distribution of liquid desorption from the surface of studied samples for individual liquids were determined, using the method described in papers [8, 9]. Estimation of surface energetic heterogeneity is based on condensation approximation applied

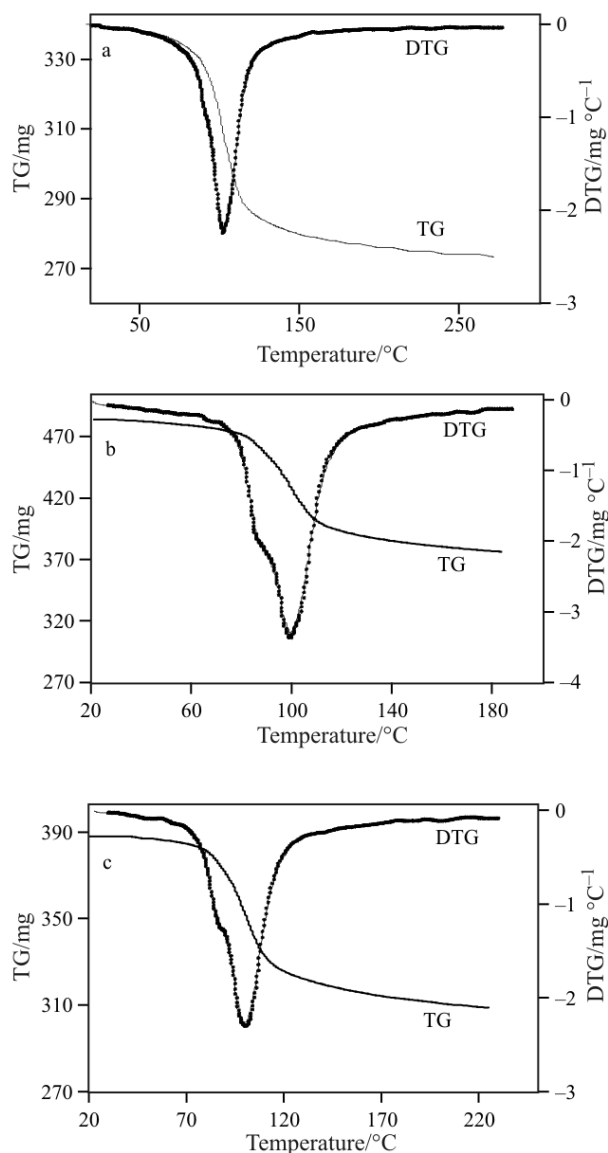


**Fig. 1** The Q-TG and Q-DTG curves of water thermodesorption from the surfaces: a – pure Al<sub>2</sub>O<sub>3</sub>, b – modified with Mn<sup>2+</sup>, c – modified with Ni<sup>2+</sup>

for description of desorption kinetics under the non-isothermal conditions (quasi-isothermal). The function of desorption energy distribution,  $\rho_n(E)$  can be calculated from the curves Q-TG and Q-DTG describing desorption kinetics [8]. Final expression for calculating the function of desorption energy distribution  $\rho_n(E)$  can be written as follows:

$$\rho_n(E) = -\frac{d\theta}{dT} \frac{1}{T} \quad (1)$$

where  $\theta$  – degree of surface coverage,  $T$  – desorption temperature.

Equation (1) was used for calculating the function of desorption energy distribution of water, benzene and *n*-octane from the aluminium oxide surface modified with cations for a given temperature  $T$  from the curves

Q-TG and Q-DTG. From the experimental data in Fig. 1 and using the above dependence, the functions of desorption energy distribution presented in Fig. 2 were calculated for the individual studied systems.

High degree of nonlinearity of the above curves of the dependences calculated from Eq. (1) results from large energetic heterogeneity of the surface of studied samples. Table 2 presents the values of parameters describing energetic heterogeneity for the individual studied samples: range of changes in the desorption energy  $\Delta E_d$  (in  $\text{kJ mol}^{-1}$ ), values of desorption energy corresponding to the peak maximum,  $E_d^{\text{max}}$  (in  $\text{kJ mol}^{-1}$ ) and maximal values of the derivative of the number of active centres after the energy  $\rho^{\text{max}}$  (in  $\text{mol kJ}^{-1}$ ). The functions of desorption energy distribution of the samples modified with  $\text{Mn}^{2+}$  and  $\text{Ni}^{2+}$  ions differ in size of desorption energy and shape of curves (Fig. 2).

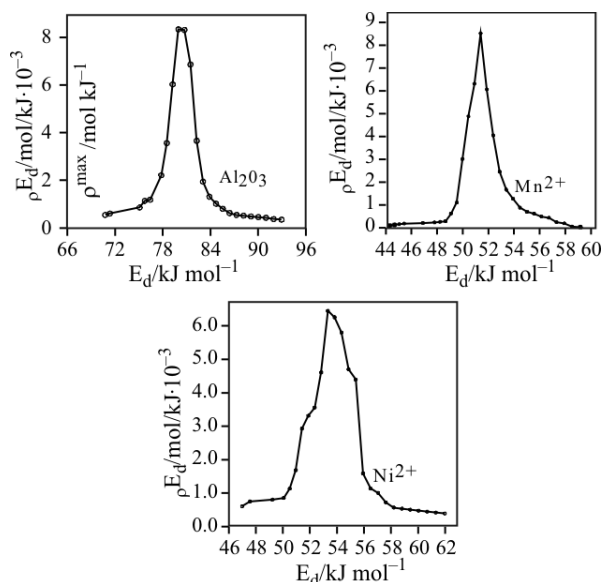


**Fig. 2** Desorption energy distribution function of water from pure and modified  $\text{Al}_2\text{O}_3$  samples

**Table 1** Properties of liquid adsorption layers on the surface of pure  $\text{Al}_2\text{O}_3$  and after modification samples

Samples	$a_{\text{water}}/\text{mmol g}^{-1}$	$n_{\text{water}}$	$a_{\text{benzene}}/\text{mmol g}^{-1}$	$n_{\text{benzene}}$	$a_{\text{n-octane}}/\text{mmol g}^{-1}$	$n_{\text{n-octane}}$
Pure $\text{Al}_2\text{O}_3$	13.5	5.8	2.57	3.1	1.51	2.2
$\text{Mn}^{2+}/\text{Al}_2\text{O}_3$	14.8	6.9	2.05	2.6	1.26	1.9
$\text{Ni}^{2+}/\text{Al}_2\text{O}_3$	13.8	6.2	2.39	3.0	1.36	2.1

**Table 2** Changes of desorption energy of the liquids from the tested samples

Samples	Water			Benzene			n-Octane		
	$\Delta E_d/\text{kJ mol}^{-1}$	$E_d^{\text{max}}/\text{kJ mol}^{-1}$	$\rho^{\text{max}}/\text{mol kJ}^{-1}$	$\Delta E_d/\text{kJ mol}^{-1}$	$E_d^{\text{max}}/\text{kJ mol}^{-1}$	$\rho^{\text{max}}/\text{mol kJ}^{-1}$	$\Delta E_d/\text{kJ mol}^{-1}$	$E_d^{\text{max}}/\text{kJ mol}^{-1}$	$\rho^{\text{max}}/\text{mol kJ}^{-1}$
Pure $\text{Al}_2\text{O}_3$	15–100	45	6.0	18–100	34	7.9	12–71	25	3.2
$\text{Al}_2\text{O}_3/\text{Mn}^{2+}$	44–59	52	8.6	53–71	59	7.5	31–41	38	2.6
$\text{Al}_2\text{O}_3/\text{Ni}^{2+}$	47–62	53	6.5	53–70	57	7.3	20–27	25.5	3.5

The calculations of desorption energy distribution function presented indicate a complex mechanism of desorption and an effect of ions on properties of aluminium oxide surface. In the case of water adsorption, a shift of desorption energy value corresponding to the peak maximum ( $E_d^{\text{max}}$ ) on the distribution curve is observed towards higher values  $E_d$ , for the samples with spread modifiers. This can be due to the effect of adsorbed cations on the aluminium oxide surface on the properties of water layer bonded with the surface (Fig. 2). The cations cause formation of a new structure of adsorption layer responsible for the increase of its thickness, but thickness decreases for benzene and *n*-octane.

Similar dependences of adsorption energy changes are found for other liquids (benzene, *n*-octane) where the value  $E_d$  for the sample with adsorbed *n*-octane is about 1.5 times as large as that for the sample  $\text{Mn}^{2+}/\text{Al}_2\text{O}_3$ , compared with the pure sample  $\text{Al}_2\text{O}_3$ . This is due to stronger interaction of *n*-octane molecules with new active centres on the surface (formation of a new structure, stiffening of adsorption film of smaller thickness).

These differences are caused by formation of new, energetically different active centres by ions affecting the mechanism of adsorption and desorption processes as well as properties of adsorption layers (thickness, structure). After modification with manganese and nickel chlorides, the aluminium oxide surface becomes more homogeneous probably due to formation of microcrystals. Properties of the new surface are a result of the influence of manganese and nickel cations, as well as chloride anions on adsorption properties and sample porosity. Modification of the surface with aluminium oxide cations reduces basic character of the adsorbent and changes adsorbate molecule interactions with its surface. However, adsorption of chloride anions masks Lewis active acidic centers.

Parameters of porosity (i.e. geometric heterogeneity) of the studied samples included in Table 3 were calculated from the adsorption–desorption isotherms of nitrogen (Fig. 3), obtained by means of sorptomate; the isotherms can be classified as type II according to BET. This type of curve results from multilayer adsorption of nitrogen. The presence of hysteresis loop on the adsorption–desorption isotherms is the evidence for the capillary condensation phenomenon. As follows from Table 3 the specific surface area calculated using the BET method decreases in the case of modification with manganese and nickel cations which results from smaller adsorption of nitrogen (Fig. 3). The values of diameter and pore volume calculated from isotherms also decrease due to formation of manganese and nickel chloride microcrystals.

Figure 4 presents pore volume distribution functions in relation to their radii for the samples modified with manganese and nickel cations calculated from the low-temperature adsorption–desorption isotherms of nitrogen (Fig. 3). The curves are typical of a Gaussian distribution with the peak maxima corresponding to the radii given in Table 3.

Thus the presence of a modifier (cation) on the surface causes insignificant decrease of fractal dimension due to increase in porosity of samples. Figures 4 and 5 show the functions of pore volume distribution towards the radii of the above mentioned samples. Generally the trend of changes of these parameters is similar to those obtained by means of sorptomate (Table 3). However, numerical values of the obtained data are different in both standard methods; this is due to the fact that the porosimetric method is a destructive method for the studying samples.

Thus the presence of a modifier (cation) on the surface causes insignificant decrease of fractal dimension due to increase in porosity of samples. Figure 5

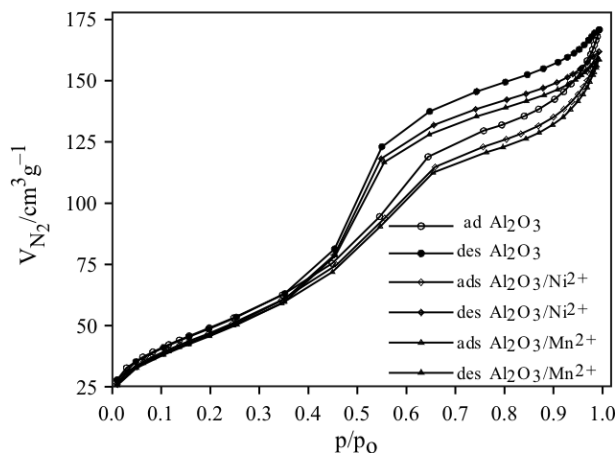


Fig. 3 Nitrogen adsorption–desorption isotherms for modified and unmodified Al<sub>2</sub>O<sub>3</sub> samples

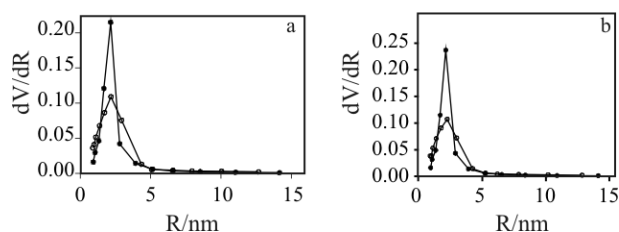


Fig. 4 Sorptometry of pore-size distribution functions of Al<sub>2</sub>O<sub>3</sub> samples modified by a) Mn<sup>2+</sup> and b) Ni<sup>2+</sup>

shows the functions of pore volume distribution towards the radii of the above mentioned samples obtained from porosimetry studies. Porosity parameters (diameter and pore volume as well as specific surface area) are collected in Tables 4 and 5 for the studied samples. Generally the trend of changes of these parameters is similar to those obtained by means of sorptomate (Table 3). However, numerical values of the obtained data are different in both standard methods; this follows from the fact that the porosimetric method is a destructive method.

**Table 3** Adsorption and structural parameters of the pure and modified aluminium oxide determined from the nitrogen adsorption isotherms

Samples	Pore diameter R/nm			Single point	Total pore volume V/cm <sup>3</sup> g <sup>-1</sup>		Specific surface area S/m <sup>2</sup> g <sup>-1</sup> BET method
	Methods				BJH (adsorption)	BJH (desorption)	
	BET	BJH-(ads.)	BJH-(des.)				
Pure Al <sub>2</sub> O <sub>3</sub>	5.82	4.81	4.16	0.25	0.27	0.27	174.9
Mn <sup>2+</sup> /Al <sub>2</sub> O <sub>3</sub>	5.78	4.68	4.07	0.24	0.25	0.25	164.3
Ni <sup>2+</sup> /Al <sub>2</sub> O <sub>3</sub>	5.76	4.68	4.05	0.24	0.25	0.25	167.6

**Table 4** Structural parameters of the pure and modified aluminium oxide samples determined from porosimetry method

Samples	Pore diameter R/nm	Total pore volume V/cm <sup>3</sup> g <sup>-1</sup>	Specific surface area S/m <sup>2</sup> g <sup>-1</sup>
Pure Al <sub>2</sub> O <sub>3</sub>	3.2	0.22	107.5
Mn <sup>2+</sup> /Al <sub>2</sub> O <sub>3</sub>	3.6	0.19	90.9
Ni <sup>2+</sup> /Al <sub>2</sub> O <sub>3</sub>	3.2	0.16	81.7

Loss of mass of liquid into the volume occupied by the liquid in the pores of the studied material during programmed thermodesorption was calculated from the Q-TG curves. Table 5 presents the comparison of the obtained results of calculations with the data of measurements made by means of sorptometer and porosimetry. Comparison of the above data obtained from three independent measurement techniques gives good agreement.

From the AFM data the surface fractal dimensions were calculated. They are 2.60 (pure aluminium oxide), 2.52 (modified with manganese chloride) and

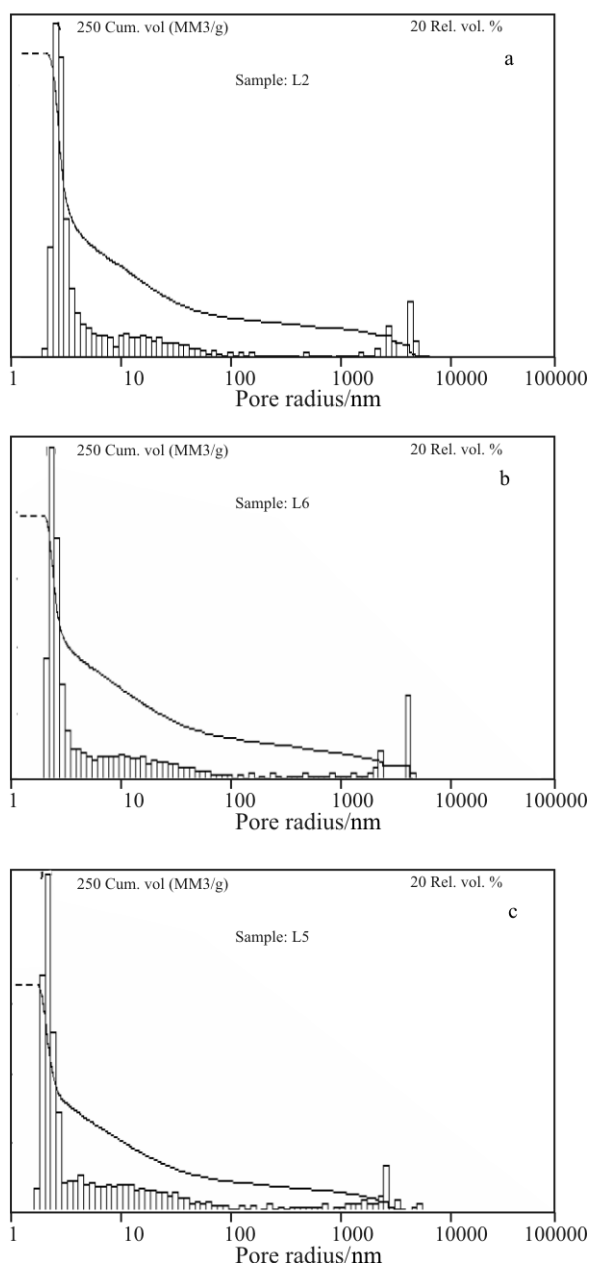


**Fig. 5** Porosimetry of pore-size distribution functions of a – pure  $\text{Al}_2\text{O}_3$ , b – modified with  $\text{Mn}^{2+}$ , c – modified with  $\text{Ni}^{2+}$

2.53 (modified with nickel chloride). The results presented in Table 5 confirm the studies of changes (decrease) of sample porosity after modification made by the use of derivatograph, sorptometer and porosimeter. From the adsorption–desorption isotherms of nitrogen, fractal dimensions were calculated from the dependence [13, 14]:

$$D_f = 3 - d[\ln a(x)] / d[\ln(-\ln x)] \quad (2)$$

where  $a$  – the adsorption value,  $x = p/p_0$ .

For the studied samples the following values of fractal dimensions were obtained using complex methods and presented in Table 6. Figure 6 shows EDX photo of the pure and modified alumina surface. There is additional illustration of the real advanced material surfaces by means of the apparatus JSM-25 JOEL type and LEO SEM 1430VP with EDX detector. From the comparison of sample images, it also follows that the surfaces after modification with cations are less porous than the pure surface.

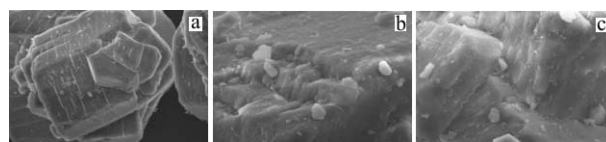
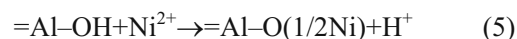


**Fig. 6** EDX photographs of the sample surface: a – pure  $\text{Al}_2\text{O}_3$ , b – modified by  $\text{Mn}^{2+}$ , c – modified by  $\text{Ni}^{2+}$

The results of EDX analysis of pure (Fig. 7) and modified (Figs 8, 9) samples based on X-ray dispersive spectra show the presence of  $\text{Cl}^-$  anions on the adsorption surface, apart from  $\text{Ni}^{2+}$  and  $\text{Mn}^{2+}$  ions. It means that  $\text{MnCl}_2$  and  $\text{NiCl}_2$  as well as  $\text{MnCl}^+$  and  $\text{NiCl}^+$  complexes reside on  $\text{Al}_2\text{O}_3$  surface.

The most probable adsorption reactions on alumina surface are:



It appears that new active centres have been created on modified surface and influence the physico-chemical properties of alumina oxide samples [15]. The % amounts of elements in studied samples are given in Table 7.

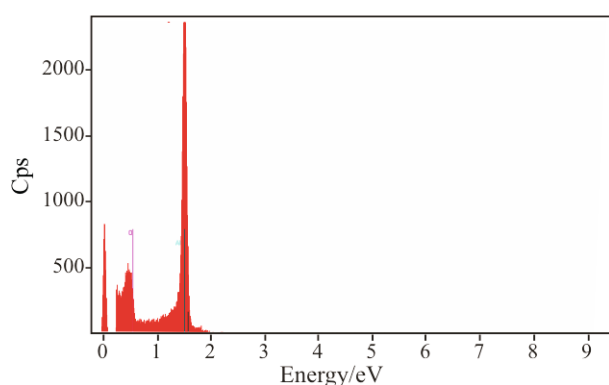
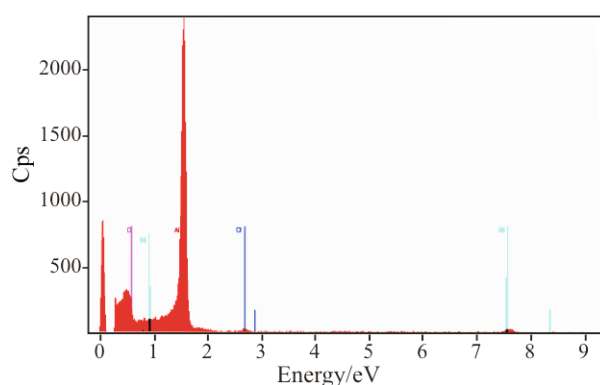
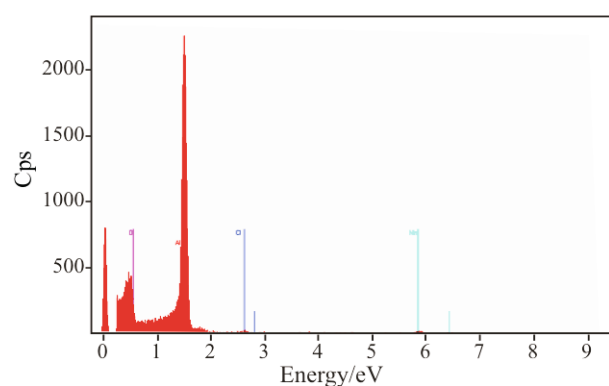
Figure 10 presents X-ray diffraction patterns for pure and modified  $\text{Al}_2\text{O}_3$ . Detailed analysis of these XRD patterns shows no substantial differences between them. It means that Mn or Ni species did not form any separate crystalline phases. So, it indicates, with high probability, that Mn and Ni are in atomic dispersion or form very small particles whose size is lower than 2 nm.

**Table 5** The comparison of the obtained pore volume results of calculations with the data of measurements made by means of thermogravimetry, sorptometry and porosimetry methods (in cm<sup>3</sup> g<sup>-1</sup>)

Samples	Thermodesorption of:			Sorptometry: Single point BHJ(ads.) BHJ(des.)		Porosi- metry
	Water	Benzene	<i>n</i> -Octane	Volume of N <sub>2</sub>		Volume of Hg
Pure Al <sub>2</sub> O <sub>3</sub>	0.25	0.25	0.28	0.25 0.27 0.26		0.22
Mn <sup>2+</sup> /Al <sub>2</sub> O <sub>3</sub>	0.27	0.20	0.23	0.24 0.25 0.25		0.19
Ni <sup>2+</sup> /Al <sub>2</sub> O <sub>3</sub>	0.26	0.23	0.26	0.24 0.26 0.25		0.16

**Table 6** Calculated of values of fractal dimensions on the basis of complex methods

Sample	Thermodesorption of:			Sorptometry	Porosimetry	AFM
	Water	Benzene	<i>n</i> -Octane			
Pure Al <sub>2</sub> O <sub>3</sub>	2.41	2.42	2.39	2.40	2.50	2.66
Mn <sup>2+</sup> /Al <sub>2</sub> O <sub>3</sub>	2.39	2.42	2.38	2.39	2.40	2.52
Ni <sup>2+</sup> /Al <sub>2</sub> O <sub>3</sub>	2.40	2.41	2.39	2.39	2.42	2.53

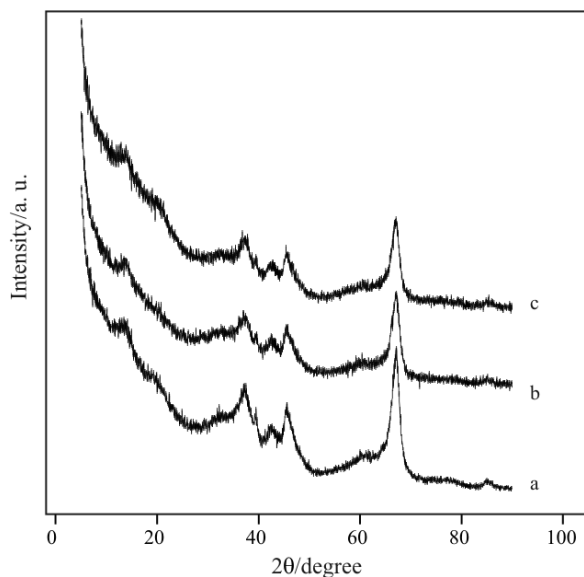
**Fig. 7** EDX spectrum of pure Al<sub>2</sub>O<sub>3</sub>**Fig. 9** EDX spectrum of Al<sub>2</sub>O<sub>3</sub>, modified by Ni<sup>2+</sup>**Fig. 8** EDX spectrum of Al<sub>2</sub>O<sub>3</sub> modified by Mn<sup>2+</sup>

## Conclusions

On the basis of the obtained results it can be concluded that the presence of cations on the surface decreases adsorption capacity of aluminium oxide compared with that of benzene and *n*-octane. Adsorption capacity of water increases with the concentration of modifiers. The greatest changes of values of water adsorption capacity were obtained for the samples of aluminium oxide with spread Mn<sup>2+</sup> and Ni<sup>2+</sup> cations of concentration  $c=0.4$  mmol g<sup>-1</sup>. These differences are caused by formation of new, energetically different active centers by ions affecting the mechanism of adsorption and desorption processes, as well as properties of adsorption layers (thickness, structure).

**Table 7** The % values of the individual atoms in the tested samples

Methods	Samples		
	Pure Al <sub>2</sub> O <sub>3</sub> % of	Mn <sup>2+</sup> /Al <sub>2</sub> O <sub>3</sub> % of	Ni <sup>2+</sup> /Al <sub>2</sub> O <sub>3</sub> % of
EDX	Al – 43.85	Al – 47.63	Al – 47.22
	O – 56.15	O – 50.30	O – 50.20
		Mn – 1.58	Ni – 2.08
		Cl – 0.48	Cl – 0.50
XRF	–	Mn – 2.30	Ni – 2.24

**Fig. 10** The XRD spectrum of: a – pure Al<sub>2</sub>O<sub>3</sub>, b – modified by Ni<sup>2+</sup>, c – modified by Mn<sup>2+</sup>

The functions of desorption energy distribution of the samples modified with Mn<sup>2+</sup> and Ni<sup>2+</sup> ions differ in size of desorption energy and shape of curves. High degree of nonlinearity of the above curves results from large energetic heterogeneity of the surface of studied samples of material. After modification with manganese and nickel chlorides, the aluminium oxide surface becomes more homogeneous probably due to formation of microcrystals. Properties of the new surface are a result of influence of manganese and nickel cations as well chloride anions on adsorption properties and sample porosity. The presence of a

modifier (cation) on the surface causes insignificant decrease of fractal dimension due to increase in porosity of samples.

The comparison of the obtained results of calculations with the data of measurements made by means of complex methods was made. Comparison of adsorption and porosity parameters obtained from independent techniques gives good agreement.

## References

- 1 S. J. Teichner, *Bul. Soc. Chim. Fr.*, 7–8 (1974) 1226.
- 2 J. Deng, Z. Cao and B. Zhou, *Appl. Catal. A: General*, 132 (1995) 9.
- 3 M. N. Ramsis, Ch. A. Philip, M. Abd El Khlik and E.R. Souaya, *J. Thermal Anal.*, 46 (1996) 1775.
- 4 E. Kis, R. Marinkovic-Neducin, G. Lomic, G. Boskovic, D. Z. Obadovic, J. Kiurski and P. Putanov, *Polyhedron*, 17 (1998) 27.
- 5 D. Franquin, S. Monteverdi, S. Molina, M. M. Betahar and Y. Fort, *J. Mater. Sci.*, 34 (1999) 4481.
- 6 B. Grzybowska-Świerkosz, *Elementy katalizy heterogenicznej (Elements of heterogeneity catalysis)*, PWN, Warszawa 1993.
- 7 B. B. Popowski, *Nauka (Novosibirsk)*, 61 (1976) 16.
- 8 D. Sternik, P. Staszczuk, G. Grodzicka, J. Pękalska and K. Skrzypiec, *J. Therm. Anal. Cal.*, 77 (2004) 171.
- 9 A. K. Khattak, M. Afzal, M. Saleem, G. Yasmeen and R. Ahmad, *Colloids Surf. A: Physicochem. Engin. Aspects*, 162 (2000) 99.
- 10 J. Deng, Z. Cao and B. Zhou, *Appl. Catal. A: General*, 132 (1995) 9.
- 11 A. Braithwaite and M. Cooper, *Chromatographia*, 429 (1996) 77.
- 12 P. Staszczuk, M. Płanda-Czyż, D. Sternik, M. Błachnio, G. Grodzicka, J. Pękalska, S. Wasak and K. Pilorz, *J. Therm. Anal. Cal.*, 85 (2006) 339.
- 13 A. L. McClellan and H. F. Harnsberger, *J. Colloid Interface Sci.*, 23 (1967) 577.
- 14 P. Staszczuk, V. V. Kutarov and M. Płanda, *J. Therm. Anal. Cal.*, 71 (2003) 445.
- 15 P. Staszczuk, D. Sternik and V. V. Kutarov, *J. Therm. Anal. Cal.*, 69 (2003) 23.
- 16 B. Kasprzyk-Hoedern, *Adv. Coll. Interface Sci.*, 110 (2004) 19.

DOI: 10.1007/s10973-008-9369-4